Evolution of Photosynthesis: Time-Independent Structure of the Cytochrome b 6 f Complex †

ARTICLE *in* BIOCHEMISTRY · JUNE 2004

Impact Factor: 3.02 · DOI: 10.1021/bi049444o · Source: PubMed

BIOCHEMISTRY

 Volume 43, Number 20 May 25, 2004

Current Topics

Evolution of Photosynthesis: Time-Independent Structure of the Cytochrome b_6f Complex†

William A. Cramer,* Huamin Zhang, Jiusheng Yan, Genji Kurisu,‡ and Janet L. Smith

Department of Biological Sciences, Lilly Hall of Life Sciences, 915 West State Street, Purdue University, West Lafayette, Indiana 47907-2054

Received March 22, 2004; Revised Manuscript Received April 7, 2004

ABSTRACT: Structures of the cytochrome b_6f complex obtained from the thermophilic cyanobacterium *Mastigocladus laminosus* and the green alga *Chlamydomonas reinhardtii*, whose appearance in evolution is separated by 10^9 years, are almost identical. Two monomers with a molecular weight of 110 000, containing eight subunits and seven natural prosthetic groups, are separated by a large lipid-containing "quinone exchange cavity". A unique heme, heme *x*, that is five-coordinated and high-spin, with no strong field ligand, occupies a position close to intramembrane heme b_n. This position is filled by the *n*-side bound quinone, Q_n, in the cytochrome bc_1 complex of the mitochondrial respiratory chain. The structure and position of heme *x* suggest that it could function in ferredoxin-dependent cyclic electron transport as well as being an intermediate in a quinone cycle mechanism for electron and proton transfer. The significant differences between the cyanobacterial and algal structures are as follows. (i) On the *n*-side, a plastoquinone molecule is present in the quinone exchange cavity in the cyanobacterial complex, and a sulfolipid is bound in the algal complex at a position corresponding to a synthetic DOPC lipid molecule in the cyanobacterial complex. (ii) On the *p*-side, in both complexes a quinone analogue inhibitor, TDS, passes through a portal that separates the large cavity from a niche containing the Fe_2S_2 cluster. However, in the cyanobacterial complex, TDS is in an orientation that is the opposite of its position in the algal structure and bc_1 complexes, so its headgroup in the *M. laminosus* structure is 20 Å from the Fe_2S_2 cluster.

In oxygenic photosynthesis carried out by cyanobacteria, algae, and higher plants, the multisubunit cytochrome b_6f integral membrane protein complex mediates electron transfer between the photosystem II, in which H_2O is the electron donor, and the photosystem I reaction centers (Figure 1). Consistent with a basic paradigm of membrane energy transduction (*1*), electron transfer through the b_6f complex is coupled to proton translocation across the membrane. The transfer of protons across the b_6f complex, utilizing oxidation and reduction of lipophilic quinone, establishes a proton electrochemical potential gradient ($\Delta\tilde{\mu}_H{}^+$) that is negative (*n*) on the stromal side of the membrane and positive (*p*) on the lumen side. The many biochemical and biophysical studies of the complex that formed the basis for these studies, reviewed or discussed in refs *2*−*6*, formed the basis for the publication in the fall of 2003 of X-ray structures of the b_6f

† The studies reported in this review were supported by NIH Grant GMS-38323 (W.A.C.) and a fellowship from The Japanese Ministry of Education (G.K.).

* To whom correspondence should be addressed. Telephone: (765) 494-4956, Fax: (765) 496-1189. E-mail: wac@bilbo.bio.purdue.edu.

‡ Current address: Department of Life Sciences, Graduate School of Arts and Sciences, University of Tokyo, Komaba 3-8-1, Meguro, Tokyo 153-8902, Japan.

10.1021/bi049444o CCC: $27.50
Published on Web 05/04/2004

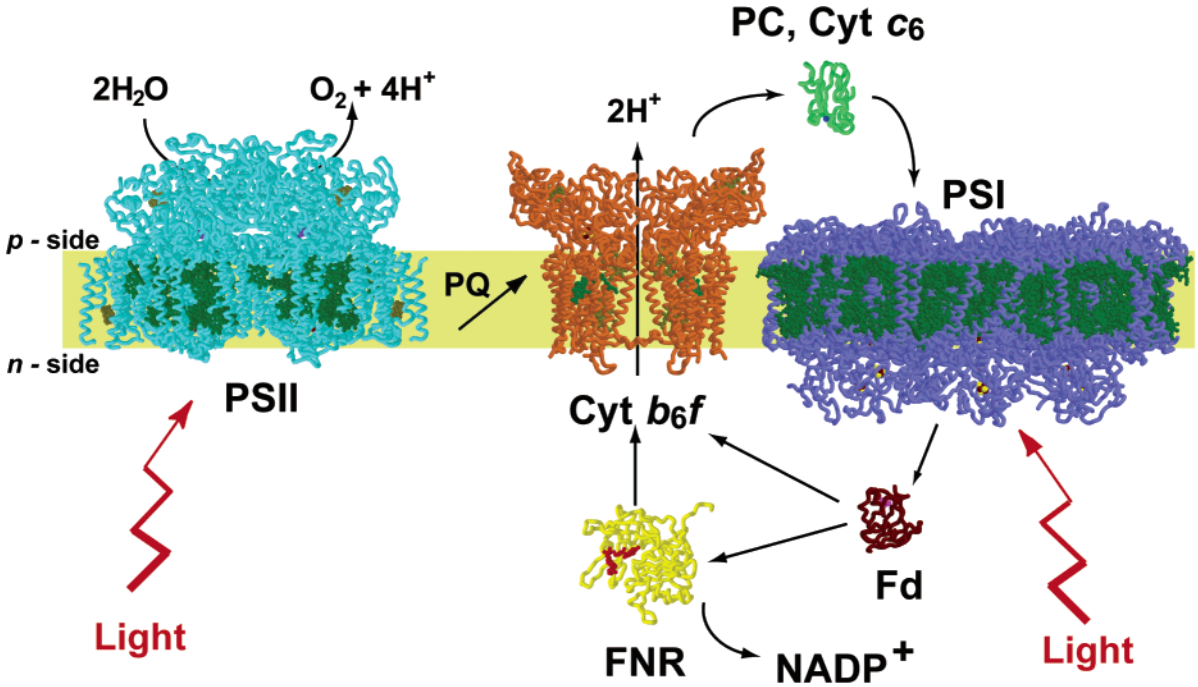

FIGURE 1: Pathway of the electron transfer−proton translocation chain in membranes that function in oxygenic photosynthesis. The structures of PSI (PDB entry 1JBO) and PSII (PDB entry 1IZL) from *Synechococcus elongatus* are shown in purple and cyan, respectively. The cytochrome b_6f complex from *M. laminosus* is shown in orange. Lumen (*p*) and stromal (*n*) side soluble electron transfer proteins are plastocyanin (green) or cytochrome c_6, ferredoxin (dark brown), and ferredoxin:$NADP^+$ reductase (yellow). The proposed pathway of cyclic electron transfer involving ferredoxin and FNR is shown.

complex from the thermophilic cyanobacterium *Mastigocladus laminosus* (*7*) (PDB entry 1UM3) and the green alga *Chlamydomonas reinhardtii* (*8*) (PDB entry 1Q90). A structure obtained in the presence of the quinone analogue inhibitor tridecylstigmatellin (TDS)[1] was at a similar resolution (3.0−3.1 Å) from both sources. Structures at a somewhat lower resolution (3.4 Å) were obtained from *M. laminosus* of (a) the native complex and (b) the complex in the presence of the quinone analogue inhibitor DBMIB.

The cytochrome b_6f complex, which carries out electron transfer coupled to proton translocation, is a dimer with a molecular weight of 220 000. It contains eight different transmembrane polypeptides; three of these polypeptide subunits bind electron transfer cofactors: cytochrome b_6 (two *b* hemes and newly discovered heme *x*), cytochrome *f* (*c*-type heme), and the Rieske iron−sulfur protein (Fe_2S_2 cluster).

With the spectroscopic observation of oxidant-induced reduction of cytochrome *b* in the cytochrome *bc* complex as a basis (*9*−*11*), models for electron transfer and proton translocation involving a semiquinone intermediate have been proposed to describe the general aspects of the electron and proton transfer reactions (*12*−*22*) One of these models, the "Q cycle", is summarized in reactions 1−7 below. The distinctive features of this model for the cytochrome b_6f complex are as follows: a *p*-side binding niche for reduced plastoquinol (PQH_2), the electron and proton donor to the complex; a high-potential electron transfer chain from PQH_2 through the ISP, to cytochrome *f* (eqs 1 and 2); a transfer of two protons from PQH_2 to the *p*-side aqueous phase for each electron transferred to the high-potential chain (eqs 2 and 3); a low-potential electron transfer chain in which the second electron from PQH_2 is transferred to *p*-side heme b_p (eq 3) and then across the membrane bilayer to *n*-side heme b_n (eq 4); and an *n*-side binding niche for PQ, which is reduced and protonated to PQH_2 in two one-electron steps (eqs 5 and 6) or in one two-electron step (eq 7).

The Q cycle describing redox changes of PQ/PQH_2 ($E_m \approx 100$ mV) is completed by *n*-side reduction of a PQ that diffuses from the *p*-side quinone site or from the membrane bilayer. The physical and chemical details of individual Q cycle reactions will not be discussed here. Electrons leave the complex via oxidation of cytochrome *f* ($E_m \approx 370$ mV) by plastocyanin or cytochrome c_6 (Figure 1), which transfers electrons through the *p*-side aqueous phase to photosystem I.

p-side quinol oxidation:

$$PQH_2 + FeS(ox) \rightarrow PQH^{\bullet} + Fe_2S_2(red)\cdot H^+ \quad (1)$$

$$Fe_2S_2(red)\cdot H^+ + \text{heme } f(ox) \rightarrow Fe_2S_2(ox) + \text{heme } f(red) + H^+_{p-side} \quad (2)$$

$$PQH^{\bullet} + \text{heme } b_p(ox) \rightarrow PQ + \text{heme } b_p(red) + H^+_{p-side} \quad (3)$$

transmembrane electron transfer:

$$\text{heme } b_p(red) + \text{heme } b_n(ox) \rightarrow \text{heme } b_p(ox) + \text{heme } b_p(red) \quad (4)$$

[1] Abbreviations: E_m, midpoint oxidation−reduction potential; DBMIB, 2,5-dibromo-3-methyl-6-isopropyl-*p*-benzoquinone; DOPC, dioleoylphosphatidylcholine; EPR, electron paramagnetic resonance; FNR, ferredoxin:$NADP^+$ reductase; ISP, iron−sulfur protein; PQ, plastoquinone; TDS, tridecylstigmatellin; Vis, visible.

n-side quinol reduction:

$$\text{heme } b_n(\text{red}) + \text{PQ} \rightarrow \text{heme } b_n(\text{ox}) + \text{PQ}^{\bullet -} \quad (5)$$

$$\text{heme } b_n(\text{red}) + \text{PQ}^{\bullet -} + 2\text{H}^+_{n-\text{side}} \rightarrow \text{heme } b_n(\text{ox}) + \text{PQH}_2 \quad (6)$$

Reactions 5 and 6 illustrate the *n*-side uptake of two protons and the two-electron reduction of PQ as two one-electron reactions. The *n*-side quinone reduction could also occur by cooperative transfer of two electrons from the two *b* hemes (*23*). This would lower the energy barrier for quinone reduction that would exist if it proceeded through a semiquinone intermediate:

$$\text{PQ} + \text{heme } b_p(\text{red}) + \text{heme } b_n(\text{red}) + 2\text{H}^+ \rightarrow \text{PQH}_2 \quad (7)$$

The Q cycle model for electron and proton transfer in the cytochrome b_6f complex described by eqs 1−7 is, to a significant extent, based on analogy with the bc_1 complex. The reactions supported by data directly obtained for reactions of the b_6f complex are (i) oxidant-induced reduction (reactions 1, 3, and 4) (*24*) and (ii) the stoichiometry of two protons per electron transferred through the high-potential chain for proton translocation across the complex (reactions 2 and 3). The details of all reactions involving semiquinone are at least somewhat conjectural at present. It has recently been proposed for the bc_1 complex that the quinol oxidation described in reactions 1 and 3 above might occur through a concerted two-electron oxidation (*25*).

Prior to the determination of the structure of the b_6f complex, crystal structures of the cytochrome bc_1 complex from the respiratory chain of bovine (*26*−*29*), avian (*27*), and yeast (*30*) mitochondria were obtained. This review will emphasize recent progress in describing the structure of the cytochrome b_6f complex. One of the consequences of the recently completed structure studies on the cytochrome b_6f complex is a better understanding of some aspects of the mechanism of electron-coupled proton translocation across the complex and the membrane. Inevitably, the new structure information has also raised new questions about some structure−function aspects of the complex.

Purification and Crystallization of the Complex

The pace of membrane protein structure determination has been very slow compared to that of soluble proteins. For example, the structural database currently contains approximately 22 000 protein structures but, at this time, only approximately 60 structures of independently determined integral membrane protein complexes (*31*, *32*) and only 10 hetero-oligomeric complexes at 3.0 Å resolution or better.

Purification to a stable, monodisperse state has been the bottleneck to both biochemical characterization and determination of structures of membrane proteins. The primary purification problem is the hydrophobic/amphiphilic property of membrane proteins, which tend to aggregate when removed from the lipid bilayer of the native biological membrane. A solvent system must be established to stabilize, purify, and crystallize each membrane protein. Detergents are excellent solubilizing agents and are used to isolate and manipulate membrane proteins (*33*). Once a membrane protein is extracted from the lipid bilayer into detergent solution, the hydrophobic domains are covered by detergent micelles. However, the detergent micelle exerts much less lateral pressure on the protein than does a lipid bilayer (*34*). This may increase the lability of detergent-solubilized membrane proteins, particularly of membrane−protein complexes (*34*−*36*). The resulting heterogeneity of the protein−detergent complex may impede both biochemical study and crystallization (*37*).

Instability frustrated crystallization of the cytochrome b_6f complex from the thermophilic cyanobacterium *M. laminosus*. The detergent-solubilized complex was susceptible to proteolysis. The earliest crystals, which diffracted poorly, grew slowly from proteolyzed protein (*38*). It was subsequently discovered by thin layer chromatographic analysis of the lipid content that the purified complex contained fewer than 0.5 molecule of lipid per monomer. Addition of pure synthetic lipid [dioleoylphosphatidylcholine (DOPC)] to the purified complex resulted in rapid, i.e., overnight, growth of diffraction-quality crystals of the unproteolyzed complex (*39*). The lipid stabilized the complex even though its headgroup is not native to cyanobacteria (*40*) and chloroplast thylakoid membranes (*41*). Thus, the purified b_6f complex of *M. laminosus* was overpurified with respect to lipid content. The instability of the complex, which prevented crystallization, was apparently caused by delipidation. The successful crystallization of the complex from *M. laminosus* was mainly a consequence of the large increase in the rate of crystallization. Delipidation was not a problem for the b_6f complex from *C. reinhardtii*. Unlike *M. laminosus*, *C. reinhardtii* can be manipulated genetically, and a polyhistidine tag was engineered at the C-terminus of cytochrome *f*, which substantially reduced the purification time.

Structure of the Cytochrome b_6f Complex

Structure Analysis of Integral Membrane Proteins. The bacterial photosynthetic reaction center was the first integral membrane protein complex whose structure was determined at high resolution from three-dimensional crystals (*42*). Many of the ∼60 integral membrane protein complexes that have been determined in the ensuing two decades carry out functions of photosynthetic or respiratory electron transport. Protein complexes from energy-transducing membranes dominate the set of determined membrane protein structures because of the relative ease of measurement of their activities through redox-linked absorbance changes in the visible spectral region. The bound chromophores essential for electron transport and the relative abundance of these proteins in the energy-transducing membrane facilitate both purification and crystallization.

Features of the Cytochrome b_6f Complex. The novel crystal structures of the b_6f complex from the thermophilic cyanobacterium *M. laminosus* (*7*) and from the green alga *C. reinhardtii* (*8*) provide a structural framework for extensive biochemical data. Here we emphasize the major conclusions about structure and function, which are nearly identical for the two b_6f structures from the two sources. Although the appearance of cyanobacteria and green algae in evolution is separated by approximately 10^9 years, the structures are very similar, as expected from the high level of sequence identity (>60% for the four large protein subunits). Therefore, the

Table 1: Subunits and Masses of the Cytochrome b_6f Complex from *M. laminosus* Measured by Electrospray Ionization Mass Spectrometry (*43*)

subunit	mass (Da)	
	calculated	measured
PetA (cyt *f*)	32270	32270
PetB (cyt b_6)	24884	24710
PetC (Rieske iron−sulfur protein)	19202	19295
PetD (subunit IV)	17522	17528
PetG	na[a]	4057
PetM	3842	3841
PetL	3530	3530
PetN	3304	3304
total mass of the monomer	na[a]	108535

[a] Not applicable.

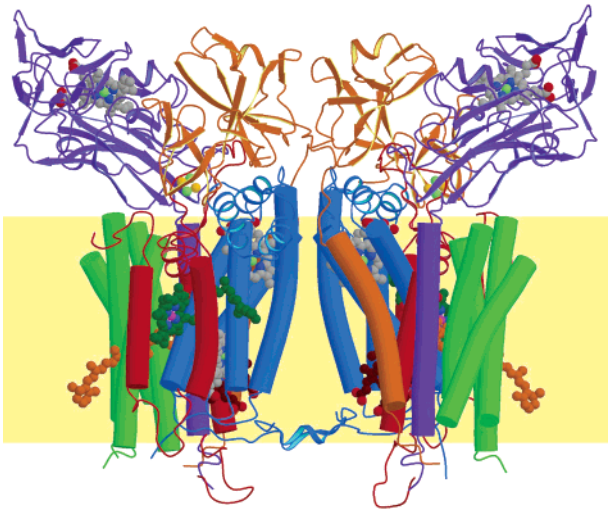

FIGURE 2: Side view of the cytochrome b_6f complex from the thermophilic cyanobacterium *M. laminosus*. The overall dimensions of the dimer in this profile are 100 Å × 120 Å. The color code is as follows: blue for cytochrome b_6, red for subunit IV, purple for cytochrome *f*, orange-brown for ISP, and green for PetG, -L, -M, and -N. Prosthetic groups displayed in space-filling diagrams are heme *f*, b_p, and b_n (gray), heme *x* (dark red), chlorophyll (green), and β-carotene (orange-brown). The membrane bilayer is shown in yellow.

conclusions drawn from these two structures also should apply to b_6f complexes from higher plants, which share the high level of sequence identity. Given the presently modest diffraction limits of the crystals, some details differ in the two crystal structures and are not discussed here.

The cytochrome b_6f complex is organized as a dimer containing 26 transmembrane helices. The monomer unit consists of eight polypeptide subunits, the large cytochrome *f* (*petA* gene product), cytochrome b_6 (PetB), Rieske ISP (PetC), and subunit IV (PetD) subunits and the small PetG, PetL, PetM, and PetN subunits (Table 1 and Figure 2). The functions of the four small subunits are unknown. As in other integral membrane protein complexes, the small subunits may provide structural support, here arranged as a "picket fence" at the lateral boundary of the dimer, or perhaps as a set of "chaperone" peptides that guide the assembly of the complex. Except for that of the cytochrome b_6 subunit, the measured and calculated subunit masses of the cyanobacterial complex match well (*43*). The profile of the b_6f complex viewed from the side (Figure 2) shows that, unlike the dimeric mitochondrial bc_1 complex, significant extension of the complex from the membrane bilayer occurs only on the *p*-side, through the soluble domains of cytochrome *f* and the ISP. On the *n*-side of the complex, the aqueous phase contains only short loops and tails of transmembrane domains. In the crystal structure of the cyanobacterial b_6f complex, several terminal residues are disordered on the *n*-side in most of the subunits.

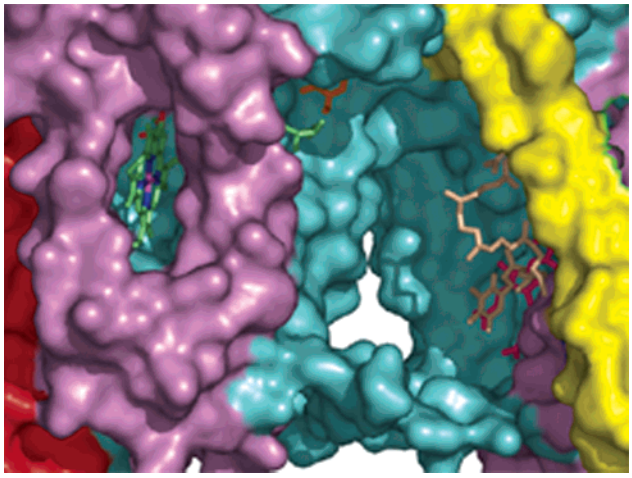

FIGURE 3: Molecular surface of the quinone exchange cavity. The color code is as follows: cyan for cytochrome b_6, violet for subunit IV, and yellow for ISP. Molecules shown as sticks are heme *x* (hot pink), plastoquinone (wheat), chlorophyll *a* (lime), and TDS (orange).

Transmembrane Helices. The eight subunits of each monomer unit span the membrane 13 times (four spans in cytochrome b_6, three in subunit IV, and one each contributed by cytochrome *f*, the ISP, and the four small subunits). In both the cyanobacterial and algal complexes, the long, 27-residue transmembrane helix of the ISP has an oblique orientation relative to the membrane normal, resulting in a domain swap in which the soluble domain associates with one monomer and the transmembrane domain with the other monomer. This is one principle by which the dimer is stabilized, as in the mitochondrial bc_1 complex, where this was first noted (*27*).

Prosthetic Groups. In both the cyanobacterium and the green alga, each monomer of the complex contains seven natural prosthetic groups: four hemes (one *c*-type, two *b*-type, and one new heme), one [2Fe-2S] cluster, one chlorophyll *a*, and one β-carotene. In addition, the cyanobacterial b_6f complex also contains one molecule of bound plastoquinone near heme b_n, and a sulfolipid was detected in the algal complex at the position of an artificial lipid on the *p*-side of the cyanobacterial complex.

Quinone Exchange Cavity. The two monomers enclose a large cavity (30 Å high × 25 Å wide × 15 Å deep) that appears to be a quinone exchange cavity (Figure 3). The walls of the cavity are formed by the C, D, and F helices of one monomer and the A, E, and ISP transmembrane helices of the other, and the *n*-side floor of the cavity is formed by the 25 N-terminal residues of cytochrome b_6. The *p*-side roof is formed by helices "cd1" and "cd2" (between transmembrane helices C and D) of cytochrome b_6. Plastoquinol, with a lipophilic long chain (nine isoprenoids and 45 carbons), donates a hydrogen to the complex (eqs 1−3). Quinol−quinone exchange occurs between the bulk hydrophobic

phase of the lipid bilayer and the proton and electron acceptor sites on the *p*- and *n*-sides of the membrane. Both of these sites are accessible only through the quinone exchange cavity.

Structural Struts. In vivo, the cavity is almost certainly filled with lipid. In the structure of the *M. laminosus* b_6f complex, two well-defined molecules of the foreign lipid DOPC, addition of which was necessary for crystallization (*39*), appear to act as structural struts for the cavity (*7*). The great facilitation of the crystallization by added lipid is likely a consequence of the reduced structural heterogeneity in the purified delipidated complex, perhaps arising from collapse of the cavity in the delipidated complex. The *n*-side of the cavity of the *C. reinhardtii* b_6f complex contains a sulfolipid at a position similar to that of the *n*-side DOPC molecule in the *M. laminosus* complex.

n-Side of the Cavity. The most striking feature in the b_6f complex is a unique heme, which occupies a site filled by ubiquinone in the bc_1 complex, adjacent to heme b_n. This heme is covalently linked by a single thioether bond to an invariant Cys35 on the *n*-side of helix A of cytochrome b_6. The unprecedented heme is tentatively designated heme *x* (heme c_i by Stroebel *et al*.) because of the single thioether cross-link and the absence of any orthogonal amino acid ligand (*7*, *8*). Heme *x* is inferred to be ubiquitous in b_6f complexes because of the invariance of Cys35 and numerous residues that border the heme. Mutagenesis of Cys35 to Val in *C. reinhardtii* (*44*) or to Ser in the cyanobacterium *Synechococcus* sp. 7002 (J. Yan and W. A. Cramer, unpublished data) resulted in an unassembled complex or cell lethality. A cysteine seemingly homologus to Cys35 is present in Gram-positive bacteria such as *Bacillus subtilis*, which contains a nonphotosynthetic complex similar to cytochrome b_6f, and a cysteine residue seemingly homologous to Cys35 (*45*).

On the cavity side of the cyanobacterial complex, the closest potential heme *x* Fe ligand is the plastoquinone ring oxygen at a distance of 7 Å. In both the cyanobacterial and algal b_6f complexes, electron density on the heme b_n side of heme *x* was ascribed to a water or hydroxyl ligand, which is hydrogen-bonded to a propionate oxygen of heme b_n. This ligand has been confirmed by resonance Raman spectroscopy (*44*). In the algal b_6f complex, an additional water bridges the heme b_n propionate and its His100 ligand. Hemes *x* and b_n are in van der Waals contact. Thus, electron coupling must exist between heme b_n and heme *x*, and rapid electron transfer between them seems to be inevitable. The direction and rate of this electron transfer are unknown at present, partly because there is no precise information about the E_m of heme *x*. The spectroscopic observation of a component resembling heme *x* indicated that it has an E_m similar to that of heme b_n (*46*). However, resonance Raman spectra imply that the valence of the iron is Fe^{2+}, although this may be a consequence of photoreduction (*44*). The answer to the question of why heme *x* was never detected spectroscopically, considering the millions of light flashes that have been incident on the b_6f complex over the past 40 years, lies in the broad low-amplitude visible spectrum that is associated with high-spin hemes (*47*), and also perhaps by coupling of its redox properties, and resulting spectra and spectral changes, to those of heme b_n. A broad low-amplitude difference spectrum of heme *x* in the complex can be detected in visible light difference spectra only when strong field orthogonal ligands such as pyridine are used (H. Zhang *et al*., unpublished data).

If the potential of heme *x* is similar to that of heme b_n ($E_m \approx -50$ mV), the *n*-side reactions of the Q cycle described in eqs 1−7 might be modified to include heme *x* in the pathway of electron transfer to PQ. The reaction described by eq 5 would be replaced by

$$\text{heme } b_n(\text{red}) + \text{heme } x(\text{ox}) \rightarrow \text{heme } b_n(\text{ox}) + \text{heme } x(\text{red}) \quad (8)$$

$$\text{heme } x(\text{red}) + \text{PQ} \rightarrow \text{heme } x(\text{ox}) + \text{PQ}^{\bullet -} \quad (9)$$

The close coupling of hemes b_n and *x* also suggests that they may function in a cooperative two-electron reduction of PQ linked to the *n*-side proton uptake that is required for the formation of the proton electrochemical potential:

$$\text{heme } b_n(\text{red}) + \text{heme } x(\text{red}) + 2\text{H}^+ + \text{PQ} \rightarrow \text{heme } b_n(\text{ox}) + \text{heme } x(\text{ox}) + \text{PQH}_2 \quad (10)$$

Function of Heme x. From its position in the b_6f complex, heme *x* is assumed to function in all redox events involving heme b_n. This hypothesis (*7*, *8*) is that heme *x* functions in "cyclic electron transfer", which is found in photosynthetic, but not mitochondrial, membranes. This function of heme *x* is also suggested by its five-coordinate high-spin state. It is natural to consider the possibility that either PQ or ferredoxin could provide the ligand to heme *x*, although a conformational change of the complex that would allow access of ferredoxin to heme *x* is unknown. The electron transfer partner could also be ferredoxin:$NADP^+$ oxidoreductase in higher plants (*48*). Binding of negatively charged ferredoxin to the stromal side surface of the b_6f complex would be facilitated by the positive *n*-side surface potential of the complex (*7*). Although heme *x* is somewhat closer to the stromal side surface of the b_6f complex than heme b_n, it is buried below a layer of protein. Although the high-spin state of heme *x* seems to be "crying for a ligand", e.g., ferredoxin, it is difficult to imagine how this could occur, although ferredoxin or ferredoxin:$NADP^+$ reductase could transfer an electron through the protein. The crystal structures of the two b_6f complexes differ in this region, and neither structure may be informative in detail. The *n*-side terminal residues of all subunits are the least well ordered regions of the cyanobacterial complex. However, in the algal complex, a major crystal lattice contact from this region may influence the conformations of these short peptides, leading to a slightly more ordered structure. The observed conformational differences in *n*-side subunit termini demonstrate the possibility for conformational changes.

n-Side Binding Site of Plastoquinone. The *M. laminosus* b_6f complex includes a bound plastoquinone molecule whose headgroup is ~4 Å from heme *x* (Figure 3). PQ forms no hydrogen bonds and few other contacts with the protein. In helix E of subunit IV, Phe40, Leu37, Tyr38, and Pro41 are in van der Waals contact with the first two isoprenoid units of PQ. The PQ site is simply a surface within the quinone exchange cavity. It is not a concave niche, as is the *n*-side quinone binding site in the cytochrome bc_1 complex (*30*, *49*), but rather an approximately flat surface of the cavity wall.

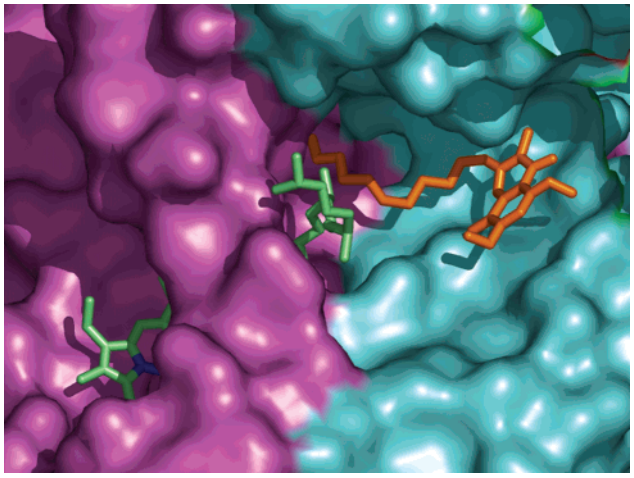

FIGURE 4: *p*-Side (11 Å × 12 Å) portal for quinone passage. The color code is like that in Figure 3: cyan for cytochrome b_6, and violet for subunit IV. Molecules shown as sticks are chlorophyll *a* (lime) and TDS (orange).

p-Side of the Cavity. Electron and proton transfers on the *p*-side of the b_6f complex occur in a Q_p site, or "Q_p pocket", that contains the Fe_2S_2 cluster of the iron−sulfur protein. PQH_2 must access the Q_p site through a small portal leading from the quinone exchange cavity (Figure 4). The Fe_2S_2 cluster-binding domain of the ISP docks into the Q_p pocket from the *p*-side aqueous phase by contacts with the cd1 and cd2 helices of cytochrome b_6 and the "ef" helical loop (between helices E and F) of subunit IV. These loops are among the most conserved regions of the b_6f complex. Despite the conservation, the Q_p pocket is narrower in the cyanobacterial than in the algal b_6f complex, due to an ∼2 Å shift of the ef helix and the C-terminal region of the E helix. The wider pocket of the algal complex allows the ISP to penetrate ∼3 Å deeper into the Q_p site.

Differences in binding of the inhibitor to cyanobacterial and algal cytochrome b_6f are consistent with the Q_p pocket differences. Both crystal structures include tridecylstigmatellin (TDS), a quinone analogue inhibitor of *p*-side electron transfer. In the *C. reinhardtii* b_6f complex, the TDS headgroup passes through the portal into the Q_p pocket, where a TDS oxygen is hydrogen bonded to His155 of the ISP. This binding mode, which clearly illustrates how TDS inhibits at the Q_p site, is similar to that of the cytochrome bc_1 binding of stigmatellin, another quinone analogue inhibitor. In contrast, TDS exhibits a novel binding orientation in the cyanobacterial b_6f complex, in which its hydrocarbon tail plugs the narrow portal and its headgroup remains in the quinone exchange cavity. Thus, crystallization trapped the two b_6f complexes in slightly different states with respect to ISP and "drug" interaction with the Q_p site. The existence of different states suggests that the Q_p pocket may alter its shape in response to binding of natural ligands such as PQ or PQH_2 and the ISP. Shape changes may facilitate movement of PQ between a subsite for electron transfer to the ISP and a subsite for electron transfer to heme b_n, which is ∼20 Å farther into the Q_p pocket than the ISP Fe_2S_2 cluster. It is impossible to know whether the shape differences in the Q_p pockets of the two crystal structures are a result of crystallization or inhibitor binding conditions. Virtually all residues within the Q_p pocket are conserved, so both of the observed pocket shapes should be accessible to both b_6f complexes. The tail-in, head-out binding mode for TDS observed in *M. laminosus* cytochrome b_6f seems to be inaccessible to the *C. reinhardtii* b_6f complex, possibly because Ala186 of the cytochrome b_6 D helix and Leu81 of subunit IV, which contact TDS in *M. laminosus*, are replaced by a Leu and Phe residue in *C. reinhardtii* (J. Yan and W. A. Cramer, in preparation).

A binding site for the quinone analogue inhibitor DBMIB was identified in difference electron density at 3.4 Å resolution from crystals of cyanobacterial cytochrome b_6f that had cocrystallized with DBMIB. The DBMIB site is far from the Q_p site and 20 Å from the Fe_2S_2 cluster. It is not apparent how DBMIB inhibits electron transfer at the cluster site that is 20 Å distant. This result should be considered in the context of studies in which more than one inhibitory DBMIB binding site was found, and the highest-affinity site had no effect on the EPR spectrum of the Fe_2S_2 cluster (*50*).

Distances between the Fe_2S_2 Cluster and Cytochrome f. In the presence of the TDS quinone analogue inhibitor, the distances of the ISP Fe_2S_2 cluster from cytochrome *f* are slightly different [25 Å (*M. laminosus*) or 28 Å (*C. reinhardtii*) from edge to edge] in the two complexes, in a manner that may relate to the different modes of binding of TDS described above. For *M. laminosus*, for which a native structure was obtained, this distance is hardly changed (≤1−2 Å in the native structure in the absence of TDS). Irrespective of the reasons for these differences, the Fe_2S_2 cluster is too far [25 Å (*M. laminosus*) or 28 Å (*C. reinhardtii*) from edge to edge] from the heme of cytochrome *f* to allow electron transfer from the ISP to cytochrome *f* at the classical rate observed *in vivo* or *in situ* of approximately 200 s^{-1}. This rate constant corresponds to that of the rate-limiting step of photosynthesis. Average rate distance coefficients [$\beta_{avg} = 1.2$ (*51*) or 1.4 $Å^{-1}$ (*52*)] are obtained from analyses of the rate calculated distance dependence of intraprotein electron transfer. The rate constants for electron transfer from the ISP to cytochrome *f* are only 10^{-2}−10^{-6} s^{-1} at 25 °C, taking into account the range of β values and ISP−cytochrome *f* heme distances. The rate constants were calculated assuming a reorganization energy of 1.0 eV, and $\Delta G° = 70$ meV (difference in the E_m values of ISP and cytochrome *f*). Thus, either the ISP or cytochrome *f* must move to close the gap for electron transfer in the high-potential chain. Significant movement of cytochrome *f* seems unlikely, considering the identical positions of cytochrome *f* in the two monomers of the b_6f dimer, apparently fixed by contacts between its large domain and the ef loop (between helices E and F) of subunit IV. Movement of the ISP seems more likely considering (i) the apparently flexible hinge region of the ISP (*53*), (ii) the known flexibility of the ISP hinge in the bc_1 complex (*54*−*56*), (iii) nonidentical positions of the two ISP subunits of *M. laminosus* (*7*), (iv) the significantly higher mobility of the ISP compared to cytochrome *f* in both the cyanobacteria and algal complex, and (v) crystal forms of the bc_1 complex in which the Fe_2S_2 cluster is positioned near (approximately 15 Å) the cytochrome c_1 heme (*27*−*29*). Mutagenesis studies of the hinge region of the ISP soluble domain in the cyanobacterium *Synechococcus* sp. PCC 7002 suggested that the required

movement of the ISP may be substantially smaller (*7*, *53*) than in the bc_1 complex (*54*, *55*).

Conservation of the Cytochrome bc Structure in Evolution

Three of the four core polypeptides of the cytochrome b_6f complex are conserved among all known cytochrome *bc* complexes. Cytochrome b_6, subunit IV, and the ISP are homologous to components of the bc_1 complex. Both sequence and structural similarity are greatest around the Q_p pocket. Beyond this, the b_6f and bc_1 complexes diverge in directions both parallel and perpendicular to the membrane plane, often to accommodate ligands not present in cytochrome bc_1. For example, in the membrane plane, no subunits in the bc_1 complex occupy sites analogous to the four small picket fence polypeptides (PetG, PetL, PetM, and PetN) that form the boundary around each monomer of the complex and bind β-carotene. In cytochrome bc_1, two to four different small subunits occupy different positions at the boundary of the complex. At the Q_n site, the b_6f complex binds heme *x*. Subunit IV diverges from the C-terminus of cytochrome *b*, its homologue in the bc_1 complex, and binds a chlorophyll *a* molecule. In the direction normal to the membrane plane, although the ISPs of cytochromes b_6f and bc_1 are homologous with virtually identical Fe_2S_2 binding domains, the membrane distal domains have major differences (*57*). Cytochromes *f* and c_1 are completely unrelated proteins, except for the five-residue sequence signature for the binding of a *c*-type heme.

New Questions

In addition to the question addressed above (Structure of the Cytochrome b_6f Complex) about the function of heme *x*, other major questions are generated by the new structures.

Function of the Dimer. The question of why membrane proteins are oligomers or dimers is often asked. In this case, there is an explanation. (a) The two monomers form the 30 Å × 25 Å × 16 Å quinone exchange cavity. As had previously been noted for the bc_1 complex, the reduction of quinone on the *n*-side of the membrane occurs in one monomer and the oxidation of quinol in the other (*26*). In this case, this is implied by the presence of a plastoquinone-(ol) bound to one monomer on the *n*-side of the cavity and a TDS inhibitor at the portal leading to the *p*-side quinone pocket in the other monomer (Figure 3).

Presence of the Chlorophyll a and β-Carotene Molecules. There is no obvious reason for the cytochrome b_6f complex to contain a chlorophyll or any other pigment molecule because the complex is part of the "dark" reactions of photosynthesis and participates in no known light reactions. However, the b_6f complex contains one molecule of chlorophyll per cytochrome *f* (*58*) that exchanges very slowly with exogenous chlorophyll (*59*). The light-induced triplet excited state of this chlorophyll is expected to produce destructive singlet state oxygen unless it is quenched. Thus, a carotenoid was sought that would avoid photodestruction of the b_6f complex by quenching excited chlorophyll states. Indeed, β-carotene was found in the b_6f complexes from spinach, a green alga, and a cyanobacterium in a stoichiometric ratio with the chlorophyll (*60*). It is of interest that the cyanobacterium *Synechocystis* sp. PCC 6803 contains a different carotenoid, eichinenone (*61*). Both the cyanobacterial structure and a green algal structure of the b_6f complex showed both chlorophyll *a* and β-carotene in the stoichiometry, one per cytochrome *f*, predicted from the biochemical analysis. However, in both structures, the β-carotene is 14 Å from the chlorophyll. This distance is much too large for quenching of the chlorophyll triplet state, but the conservation of the geometry of these pigments implies a function for each in the complex. Thus, questions about how the complex is protected from chlorophyll-mediated O_2 damage and the function of the bound chlorophyll *a* and β-carotene molecules arise.

ACKNOWLEDGMENT

We thank D. M. Kramer, T. E. Meyer and B. L. Trumpower for helpful discussions.

REFERENCES

1. Mitchell, P. (1975) The protonmotive Q cycle: A general formulation, *FEBS Lett. 59*, 137−139.
2. Rich, P. R., and Bendall, D. S. (1980) The redox potentials for the *b*-type cytochromes of higher plant chloroplasts, *Biochim. Biophys. Acta 591*, 153−161.
3. Kallas, T., and Malkin, R. (1988) Isolation and characterization of genes for cytochrome b_6f complex, *Methods Enzymol. 167*, 779−794.
4. Kallas, T. (1994) in *The Molecular Biology of Cyanobacteria* (Bryant, D. A., Ed.) pp 259−317, Kluwer Academic Publishers, Dordrecht, The Netherlands.
5. Cramer, W. A., Soriano, G. M., Ponomarev, M., Huang, D., Zhang, H., Martinez, S. E., and Smith, J. L. (1996) Some new structural aspects and old controversies concerning the cytochrome b_6f complex of oxygenic photosynthesis, *Annu. Rev. Plant Physiol. Plant Mol. Biol. 47*, 477−508.
6. Hauska, G., Schütz, M., and Büttner, M. (1996) in *Oxygenic photosynthesis: The light reactions* (Ort, D. R., and Yocum, C. F., Eds.) Kluwer Academic Publishers, Amsterdam.
7. Kurisu, G., Zhang, H., Smith, J. L., and Cramer, W. A. (2003) Structure of the cytochrome b_6f complex of oxygenic photosynthesis: tuning the cavity, *Science 302*, 1009−1014.
8. Stroebel, D., Choquet, Y., Popot, J.-L., and Picot, D. (2003) An atypical heam in the cytochrome b_6f complex, *Nature 426*, 413−418.
9. Trumpower, B. L. (1981) Function of the iron−sulfur protein of the cytochrome *b*-c_1 segment in electron transfer and energy-conserving reactions of the mitochondrial respiratory chain, *Biochim. Biophys. Acta 639*, 129−155.
10. Prince, R. C., Matsuura, K., Hurt, E., Hauska, G., and Dutton, P. L. (1982) Reduction of cytochrome b_6 and *f* in isolated plastoquinol-plastocyanin oxidoreductase driven by photochemical reaction centers from *Rhodopseudomonas sphaeroides*, *J. Biol. Chem. 257*, 3379−3381.
11. Wikström, M. K. F., and Berden, J. A. (1972) Oxidoreduction of cytochrome *b* in the presence of antimycin, *Biochim. Biophys. Acta 283*, 403−420.
12. Rich, P. (1984) Electron and proton transfers through quinones and cytochrome *bc* complexes, *Biochim. Biophys. Acta 768*, 53−79.
13. Girvin, M. E., and Cramer, W. A. (1984) A redox study of the electron transport pathway responsible for generation of the slow electrochromic phase in chloroplasts, *Biochim. Biophys. Acta 767*, 29−38.
14. Jones, R. W., and Whitmarsh, J. (1988) Inhibition of electron transfer and electrogenic reaction in the cytochrome *b/f* complex by 2-*n*-nonyl-4-hydroxyquinoline *N*-oxide (NQNO) and 2,5-dibromo-3-methyl-6-isopropyl-p-benzoquinone (DBMIB), *Biochim. Biophys. Acta 933*, 258−268.
15. Furbacher, P. N., Girvin, M. E., and Cramer, W. A. (1989) On the question of interheme electron transfer in the chloroplast cytochrome b_6 *in situ*, *Biochemistry 28*, 8990−8998.
16. Kramer, D. M., and Crofts, A. R. (1994) Re-examination of the properties and function of the *b* cytochromes of the thylakoid cytochrome *bf* complex, *Biochim. Biophys. Acta 1184*, 193−201.

17. Joliot, P., and Joliot, A. (1994) Mechanism of electron transfer in the cytochrome *b*/*f* complex of algae: evidence for a semiquinone cycle, *Proc. Natl. Acad. Sci. U.S.A. 91*, 1034−1038.
18. Trumpower, B. L., and Gennis, R. B. (1994) Energy transduction by cytochrome complexes in mitochondrial and bacterial respiration: The enzymology of coupling electron transfer reactions to transmembrane proton translocation, *Annu. Rev. Biochem. 63*, 675−716.
19. Berry, E. A., Guergova-Kuras, M., Huang, L.-S., and Crofts, A. R. (2000) Structure and function of cytochrome *bc* complexes, *Annu. Rev. Biochem. 69*, 1005−1075.
20. Shinkarev, V. P., Kolling, D. R. J., Miller, T. J., and Crofts, A. R. (2002) Modulation of the midpoint potential of the [2Fe-2S] Rieske iron sulfur center by Q_o occupants in the bc_1 complex, *Biochemistry 41*, 14372−14382.
21. Zu, Y., Couture, M., Kolling, D., Crofts, A. R., Eltis, L., Fee, J., and Hirst, J. (2003) Reduction potentials of Rieske clusters: Importance of the coupling between oxidation state and histidine protonation state, *Biochemistry 42*, 12400−12408.
22. Cooley, J. W., Roberts, A. G., Bowman, M. K., Kramer, D. M., and Daldal, F. (2004) The raised midpoint potential of the [2Fe2S] cluster of cytochrome bc_1 is mediated by both the Qo site occupants and the head domain position of the Fe−S protein subunit, *Biochemistry 43*, 2217−2227.
23. Crofts, A. R. (1985) in *The Enzymes of Biological Membranes* (Martonosi, A. N., Ed.) pp 347−382, Plenum Press, New York.
24. Velthuys, B. R. (1979) Electron flow through plastoquinone and cytochromes b_6 and *f* in chloroplasts, *Proc. Natl. Acad. Sci. U.S.A. 76*, 2765−2769.
25. Osyczka, A., Moser, C. C., and Dutton, P. L. (2004) Reversible redox energy coupling in electron transfer chains, *Nature 427*, 607−612.
26. Xia, D., Yu, C.-A., Kim, H., Xia, J.-Z., Kachurin, A. M., Yu, L., and Deisenhofer, J. (1997) Crystal structure of the cytochrome bc_1 complex from bovine heart mitochondria, *Science 277*, 60−66.
27. Zhang, Z., Huang, L., Shulmeister, V. M., Chi, Y. I., Kim, K. K., Hung, L. W., Crofts, A. R., Berry, E. A., and Kim, S. H. (1998) Electron transfer by domain movement in cytochrome bc_1, *Nature 392*, 677−684.
28. Iwata, S., Lee, J. W., Okada, K., Lee, J. K., Iwata, M., Rasmussen, B., Link, T. A., Ramaswamy, S., and Jap, B. K. (1998) Complete structure of the 11-subunit mitochondrial cytochrome bc_1 complex, *Science 281*, 64−71.
29. Kim, H., Xia, D., Yu, C. A., Xia, J. Z., Kachurin, A. M., Zhang, L., Yu, L., and Deisenhofer, J. (1998) Inhibitor binding changes domain mobility in the iron−sulfur protein of the mitochondrial bc_1 complex from bovine heart, *Proc. Natl. Acad. Sci. U.S.A. 95*, 8026−8033.
30. Hunte, C., Koepke, J., Lange, C., Rossmanith, T., and Michel, H. (2000) Structure at 2.3 Å resolution of the cytochrome bc_1 complex from the yeast *Saccharomyces cerevisiae* with an antibody Fv fragment, *Structure 8*, 669−684.
31. Michel, H. (2004) Membrane proteins of known structure, http://www.mpibp-frankfurt.mpg.de/michel/public/memprotstruct.html (last updated March 12).
32. White, S. (2004) Membrane proteins of known 3D structure, http://blanco.biomol.uci.edu/Membrane_Proteins_xtal.html (last updated March 5).
33. Zulauf, M. (1991) in *Crystallization of membrane proteins* (Michel, H., Ed.) pp 53−72, CRC Press, Boca Raton, FL.
34. Cantor, R. S. (1999) Lipid composition and the lateral pressure profile in bilayers, *Biophys. J. 76*, 2625−2639.
35. Landau, E. M., and Rosenbusch, J. P. (1996) Lipidic cubic phases: A novel concept for the crystallization of membrane proteins, *Proc. Natl. Acad. Sci. U.S.A. 93*, 14532−14535.
36. Pebay-Peyroula, E., and Rosenbusch, J. P. (2001) High-resolution structures and dynamics of membrane protein−lipid complexes: a critique, *Curr. Opin. Struct. Biol. 11*, 427−432.
37. Garavito, R. M., and Ferguson-Miller, S. (2001) Detergents as tools in membrane biochemistry, *J. Biol. Chem. 276*, 32403−32406.
38. Zhang, H., Huang, D., Sainz, G., Chaudhuri, B. N., Smith, J. L., and Cramer, W. A. (2000) in *8th International Congress on Crystallization of Biological Macromolecules* (DeTitta, G., *et al.*, Eds.) p 210.
39. Zhang, H., Kurisu, G., Smith, J. L., and Cramer, W. A. (2003) A defined protein-detergent-lipid complex for crystallization of integral membrane proteins: The cytochrome b_6f complex of oxygenic photosynthesis, *Proc. Natl. Acad. Sci. U.S.A. 100*, 5160−5163.
40. Murata, N., Wada, H., and Gombos, Z. (1992) Modes of fatty acid desaturation in cyanobacteria, *Plant Cell Physiol. 33*, 933−941.
41. Dorne, A.-J., Joyard, J., and Douce, R. (1990) Do thylakoids really contain phosphatidylcholine? *Proc. Natl. Acad. Sci. U.S.A. 87*, 71−74.
42. Deisenhofer, J., Epp, O., Miki, K., Huber, R., and Michel, H. (1985) Structure of the protein subunits in the photosynthetic reaction centre of *Rhodopseudomonas viridis* at 3 Å resolution, *Nature 318*, 618−624.
43. Whitelegge, J. P., Zhang, H., Taylor, R., and Cramer, W. A. (2002) Full subunit coverage liquid chromatography electrospray-ionization mass spectrometry ($LCMS^+$) of an oligomeric membrane protein complex: the cytochrome b_6f complex from spinach and the cyanobacterium, *M. laminosus*, *Mol. Cell. Proteomics 1*, 816−827.
44. de Vitry, C., Desbois, A., Redeker, V., Zito, F., and Wollman, F.-A. (2004) Biochemical and spectroscopic characterization of the covalent binding of heme to cytochrome b_6, *Biochemistry* (in press).
45. Yu, J., Hederstedt, L., and Piggot, P. (1995) The cytochrome *bc* complex (menaquinone:cytochrome *c* reductase) in *Bacillus subtilis* has a nontraditional subunit organization, *J. Bacteriol. 177*, 6751−6760.
46. Joliot, P., and Joliot, A. (1988) The low-potential electron-transfer chain in the cytochrome *b*/*f* complex, *Biochim. Biophys. Acta 933*, 319−333.
47. Meyer, T. E., and Kamen, M. D. (1982) in *Advances in Protein Chemistry* (Anfinsen, C. B., *et al.*, Eds.) pp 105−212, Academic Press, New York.
48. Zhang, H., Whitelegge, J. P., and Cramer, W. A. (2001) Ferredoxin:$NADP^+$ oxidoreductase is a subunit of the chloroplast cytochrome b_6f complex, *J. Biol. Chem. 276*, 38159−38165.
49. Gao, X., Wen, X., Esser, L., Quinn, B., Yu, L., Yu, C., and Xia, D. (2003) Structural basis for the quinone reduction in the bc_1 complex: A comparative analysis of crystal structure of mitochondrial cytochrome bc_1 with bound substrate and inhibitors at the Q_i site, *Biochemistry 42*, 9067−9080.
50. Roberts, A. G., Bowman, M. K., and Kramer, D. M. (2002) Certain metal irons are inhibitors of cytochrome b_6f complex "Rieske" iron−sulfur protein domain movements, *Biochemistry 41*, 4070−4079.
51. Gray, H. B., and Winker, J. R. (2003) Electron tunnelling through proteins, *Q. Rev. Biophys. 36*, 341−372.
52. Page, C. C., Moser, C. C., Chen, X., and Dutton, P. L. (1999) Natural engineering principles of electron tunnelling in biological oxidation−reduction, *Nature 402*, 47−52.
53. Yan, J., and Cramer, W. A. (2003) Functional insensitivity of the cytochrome b_6f complex to structure changes in the hinge region of the Rieske iron−sulfur protein, *J. Biol. Chem. 278*, 20925−20933.
54. Darrouzet, E., Valkova-Valchanova, M., and Daldal, F. (2000) Probing the role of the Fe−S subunit hinge region during Q(o) site catalysis in *Rhodobacter capsulatus* bc_1 complex, *Biochemistry 39*, 15475−15483.
55. Darrouzet, E., Valkova-Valchanova, M., Moser, C. C., Dutton, P. L., and Daldal, F. (2000) Uncovering the [2Fe2S] domain movement in cytochrome bc_1 and its implications for energy conversion, *Proc. Natl. Acad. Sci. U.S.A. 97*, 4567−4572.
56. Darrouzet, E., Moser, C. C., Leslie, P. L., and Daldal, F. (2001) Large scale domain movement in cytochrome bc_1: a new device for electron transfer in proteins, *Trends Biochem. Sci. 26*, 445−451.
57. Carrell, C. J., Zhang, H., Cramer, W. A., and Smith, J. L. (1997) Biological identity and diversity in photosynthesis and respiration: structure of the lumen-side domain of the chloroplast Rieske protein, *Structure 5*, 1613−1625.
58. Huang, D., Everly, R. M., Cheng, R. H., Heymann, J. B., Schägger, H., Sled, V., Ohnishi, T., Baker, T. S., and Cramer, W. A. (1994) Characterization of the chloroplast cytochrome b_6f complex as a structural and functional dimer, *Biochemistry 33*, 4401−4409.
59. Pierre, Y., Breyton, C., Lemoine, Y., Robert, B., Vernotte, C., and Popot, J.-L. (1997) On the presence and role of a molecule of chlorophyll a in the cytochrome b_6f complex, *J. Biol. Chem. 272*, 21901−21908.

60. Zhang, H., Huang, D., and Cramer, W. A. (1999) Stoichiometrically bound β-carotene in the cytochrome b_6f complex of oxygenic photosynthesis protects against oxygen damage, *J. Biol. Chem. 274*, 1581−1587.
61. Boronowsky, U., Wenk, S.-O., Schneider, D., Jager, C., and Roegner, M. (2001) Isolation of membrane protein sununits in their native state: evidence for selective binding of chlorophyll and carotenoid to the b_6 subunit of the cytochrome b_6f complex, *Biochim. Biophys. Acta 1506*, 55−66.

BI049444O